EPJ manuscript No.
(will be inserted by the editor)

Cross-ladder effects in Bethe-Salpeter and Light-Front equations

J. Carbonell[1] and V.A. Karmanov[2]

[1] Laboratoire de Physique Subatomique et Cosmologie, 53 avenue des Martyrs, 38026 Grenoble, France
[2] Lebedev Physical Institute, Leninsky Prospekt 53, 119991 Moscow, Russia

Abstract. Bethe-Salpeter (BS) equation in Minkowski space for scalar particles is solved for a kernel given by a sum of ladder and cross-ladder exchanges. The solution of corresponding Light-Front (LF) equation, where we add the time-ordered stretched boxes, is also obtained. Cross-ladder contributions are found to be very large and attractive, whereas the influence of stretched boxes is negligible. Both approaches – BS and LF – give very close results.

PACS. PACS-key 03.65.Pm – PACS-key 03.65.Ge – PACS-key 11.10.St

1 Introduction

In a preceding paper [1] we have proposed a new method for solving the BS equation [2] in the Minkowski space. Our approach does not make use of the transform to the Euclidean space (Wick rotation) and is applicable to an arbitrary interaction kernel. This method was first applied in [1] to obtain the ladder solutions of a scalar model with interaction Lagrangian $\mathcal{L}_{WC} = g\phi^2\chi$. For massless exchange we reproduced analytically the Wick-Cutkosky equation [3]. For massive ladder exchange our numerical results coincide with ones found in previous works based on the Wick rotation.

In the present paper we solve the BS and LF equations with a kernel given by a sum of ladder and cross-ladder graphs. This constitutes the first calculation of cross-ladder effects in both equations. We consider scalar constituents in the state with zero total angular momentum. BS equation with ladder kernel was solved in Minkowski space in [4].

Non ladder effects, within the same model, using Feynman-Schwinger representation, were considered in ref. [5]. In this work the full set of all irreducible cross-ladder graphs in a bound state calculation was included. In [6] the effect of the cross-ladder graphs in the BS framework was estimated with the kernel represented through a dispersion relation. Non ladder self-energy effects in LF equation have been incorporated in [7,8].

The plan of the paper is the following. In section 2 we sketch the method used in [1] for solving the BS equation and find the kernel corresponding to the cross-ladder Feynman amplitude. In section 3 we remind the LF equation, obtain the LF cross-ladder kernel and incorporate also two stretched box graphs. Numerical results are given in section 4. Section 5 contains some concluding remarks. Technical details of the derivation are given in appendices A, B and C.

2 Cross-ladder kernel in BS equation

The method for solving the BS equation proposed in our previous work [1] is based on projecting the original equation:

$$\Phi(k,p) = \frac{i^2}{\left[(\frac{p}{2}+k)^2 - m^2 + i\epsilon\right]\left[(\frac{p}{2}-k)^2 - m^2 + i\epsilon\right]} \times \int \frac{d^4k'}{(2\pi)^4} iK(k,k',p)\Phi(k',p) \qquad (1)$$

on the LF plane, i.e in applying to both sides of (1) the integral transform, which for the left-hand side reads

$$\int_{-\infty}^{\infty} \Phi(k+\beta\omega, p)d\beta$$

and similarly for the full right-hand side. Here ω is an arbitrary four-vector with $\omega^2 = 0$. This transformation eliminates the singularities of the BS equation. The BS amplitude in the transformed equation is then written in terms of the Nakanishi integral representation [9], which for zero angular momentum reads:

$$\Phi(k,p) = \frac{-i}{\sqrt{4\pi}} \int_{-1}^{1} dz' \int_0^{\infty} d\gamma' \times \frac{g(\gamma',z')}{\left[\gamma' + m^2 - \frac{1}{4}M^2 - k^2 - p\cdot k\, z' - i\epsilon\right]^3} \qquad (2)$$

The equation satisfied by the weight function $g(\gamma,z)$ was derived in [1] and has the form:

$$\int_0^{\infty} \frac{g(\gamma',z)d\gamma'}{\left[\gamma'+\gamma+z^2m^2+(1-z^2)\kappa^2\right]^2} = \int_0^{\infty} d\gamma' \int_{-1}^{1} dz'\, V(\gamma,z;\gamma',z')g(\gamma',z'), \qquad (3)$$

where V is a kernel given in terms of the BS interaction kernel iK by

$$V(\gamma,z;\gamma',z') = \frac{\omega\cdot p}{\pi}\int_{-\infty}^{\infty}\frac{-iI(k+\beta\omega,p)d\beta}{\left[(\frac{p}{2}+k+\beta\omega)^2-m^2+i\epsilon\right]} \times\frac{1}{\left[(\frac{p}{2}-k-\beta\omega)^2-m^2+i\epsilon\right]}, \quad (4)$$

$$I(k,p) = \int\frac{d^4k'}{(2\pi)^4}\frac{iK(k,k',p)}{\left[k'^2+p\cdot k'z'-\gamma'-\kappa^2+i\epsilon\right]^3}. \quad (5)$$

The bound state mass M enters through the parameter

$$\kappa^2 = m^2-\frac{1}{4}M^2.$$

Equation (3) is equivalent to the initial BS equation (1) and provides, for a given kernel $K(k,k',p)$, the same bound state mass M. Once $g(\gamma,z)$ is known, the BS amplitude can be restored by eq. (2). Corresponding LF wave function $\psi(k_\perp,x)$ can be easily obtained by

$$\psi(k_\perp,x) = \frac{1}{\sqrt{4\pi}}\int_0^\infty\frac{x(1-x)g(\gamma',1-2x)d\gamma'}{\left[\gamma'+k_\perp^2+m^2-x(1-x)M^2\right]^2}. \quad (6)$$

In [1] for the ladder exchange

$$K^{(L)}(k,k',p) = \frac{-g^2}{(k-k')^2-\mu^2+i\epsilon}$$

we calculated the integrals (4), (5) for the kernel V and solved equation (3). Derivation of V for the cross-ladder kernel is quite similar but more lengthy, since the kernel itself is more complicated. The cross-ladder BS kernel is

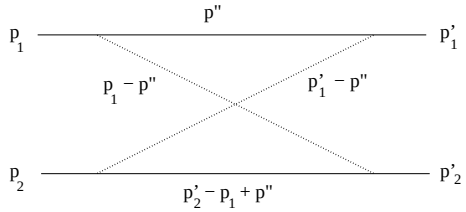

Fig. 1. Feynman cross graph.

shown in fig. 1. On mass-shell it depends on two variables: $s=(p_1+p_2)^2$ and $t=(p_1-p_1')^2$. The kernel K in the BS equation (1) is off-mass shell. It depends also on p_i^2, *i.e.*, on six scalar variables in general: $s,t,p_1^2,p_2^2,{p_1'}^2,{p_2'}^2$. One can also construct six variables, using the total momentum p and relative momenta k,k':

$$p^2,\quad k^2,\quad k'^2,\quad k\cdot k',\quad k\cdot p,\quad k'\cdot p,$$

where

$$p=p_1+p_2=p_1'+p_2',\quad k=\frac{1}{2}(p_1-p_2),\quad k'=\frac{1}{2}(p_1'-p_2').$$

In the bound state problem the value of p^2 is fixed: $p^2=M^2$.

The amplitude corresponding to the diagram in fig. 1 reads:

$$K^{(CL)}(k,k',p) = \frac{-ig^4}{(2\pi)^4}\int\frac{1}{[p''^2-m^2+i\epsilon][(p_2'-p_1+p'')^2-m^2+i\epsilon]} \times\frac{d^4p''}{[(p_1-p'')^2-\mu^2+i\epsilon][(p_1'-p'')^2-\mu^2+i\epsilon]}. \quad (7)$$

We have first to calculate this expression, substitute the result in (5), then in (4) and find in this way the cross-ladder contribution to the kernel $V(\gamma,z;\gamma',z')$ in equation (3).

The full kernel – including ladder and cross-ladder graphs – will be written in the form:

$$V(\gamma,z;\gamma',z') = V^{(L)}(\gamma,z;\gamma',z')+V^{(CL)}(\gamma,z;\gamma',z').$$

The ladder kernel $V^{(L)}$ was found in [1]. The cross-ladder contribution $V^{(CL)}$ is calculated in appendix A.

3 Ladder, cross-ladder and stretched-box kernel in LF equation

We would like to compare the results obtained in the BS approach with the equivalent ones found in Light-Front Dynamics (LFD). For this aim we precise in what follows the LF equation and derive the corresponding kernel. In the well-known variables $\boldsymbol{k}_\perp$ and x the LF equation reads (see *e.g.* [10]):

$$\left(\frac{\boldsymbol{k}_\perp^2+m^2}{x(1-x)}-M^2\right)\psi(\boldsymbol{k}_\perp,x) = -\frac{m^2}{2\pi^3}\int\psi(\boldsymbol{k}'_\perp,x')V_{LF}(\boldsymbol{k}'_\perp,x';\boldsymbol{k}_\perp,x,M^2)\frac{d^2k'_\perp dx'}{2x'(1-x')}\ . \quad (8)$$

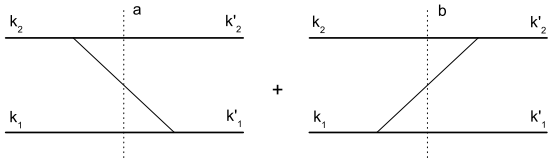

Fig. 2. Ladder LFD graphs.

The two time-ordered ladder graphs are shown in fig. 2. The corresponding kernel has the form:

$$V_{LF}^{(L)}(\boldsymbol{k}'_\perp,x';\boldsymbol{k}_\perp,x,M^2) = -\frac{4\pi\alpha\theta(x'-x)}{(x'-x)(s_a-M^2)}-\frac{4\pi\alpha\theta(x-x')}{(x-x')(s_b-M^2)}, \quad (9)$$

where

$$s_a = \frac{\boldsymbol{k}_\perp^2 + m^2}{x} + \frac{(\boldsymbol{k'}_\perp - \boldsymbol{k}_\perp)^2 + \mu^2}{x' - x} + \frac{\boldsymbol{k'}_\perp^2 + m^2}{1 - x'}$$

and

$$s_b = \frac{\boldsymbol{k'}_\perp^2 + m^2}{x'} + \frac{(\boldsymbol{k'}_\perp - \boldsymbol{k}_\perp)^2 + \mu^2}{x - x'} + \frac{\boldsymbol{k}_\perp^2 + m^2}{1 - x}.$$

The six different cross-ladder diagrams are shown in fig. 3. They have order α^2. In addition, and in the same order α^2, there are two time-ordered irreducible graphs with two mesons in the intermediate state (stretched boxes). They are shown in fig. 4. The full LFD kernel – including ladder, cross-ladder and stretched-box graphs – will be written in the form:

$$V_{LF}(\boldsymbol{k}'_\perp, x'; \boldsymbol{k}_\perp, x, M^2) = V_{LF}^{(L)} + V_{LF}^{(CL)} + V_{LF}^{(SB)}.$$

The term $V_{LF}^{(L)}$ is given by (9) and

$$V_{LF}^{(CL)} = \sum_{i=1}^{6} V_i, \quad V_{LF}^{(SB)} = \sum_{i=7,8} V_i \qquad (10)$$

are calculated in appendices B and C correspondingly.

4 Numerical results

We have solved numerically the BS equation in the form (3) and the LF equation (8) both for the ladder (L) and ladder+cross-ladder (L+CL) kernels. In the case of the LF equation (8) we added also the stretched box contributions (L+CL+SB) with two intermediate mesons shown in fig. 4. These stretched box contributions, as well as those with any number of intermediate mesons, are generated by iterations of the ladder BS kernel and are thus implicitly included in the BS approach.

The numerical procedure, based in the spline expansion of the solution, is similar to the one used in [1]. By expanding the solution $g(\gamma, z)$ on a spline basis we obtain a matrix equation:

$$\lambda B(M) g = A(M, \alpha) g. \qquad (11)$$

Like in [1], the matrix $B(M)$ was regularized by adding to its diagonal a small value $\varepsilon \sim 10^{-4} \div 10^{-12}$ and we have checked the stability of the eigenvalus relative to ε. The difference with respect to the ladder kernel is that the coupling constant α does not appear linearly in the right-hand side of (11). For a fixed mass M, the eigenvalue λ is calculated for different values of α and the value corresponding to $\lambda = 1$ can be easily extrapolated from the almost linear behaviour of $\lambda(\alpha)$.

The binding energy B as a function of the coupling constant α is shown in figures 5 and 6 for exchange masses $\mu = 0.15$ and $\mu = 0.5$ respectivley and unit constituent mass ($m = 1$). Corresponding numerical values are given in table 1. Obtaining this results is quite a lengthy numerical task, entirely due to the evaluation of the 4-dimensional integral required in the CL kernel. This fact makes difficult – though straightforward – to reach the same accuracy than for the ladder case. The results in table 1 have been obtained with $N \approx 10$ gauss quadrature points in each integration variable ensuring an accuracy of 1%.

We see that for the same kernel – ladder or (ladder + cross-ladder) – and exchange mass – $\mu = 0.15$ or $\mu = 0.5$ – the binding energies obtained by BS and LFD approaches are very close to each other. The BS equation is slightly more attractive than LFD. At the same time, the results for ladder and (ladder +cross-ladder) kernels considerably differ from each other. The effect of the cross-ladder is strongly attractive. Though the stretched box graphs are included, its contribution to the binding energy is smaller than 2% and attractive as well. This agrees with the direct calculation of the stretched box contribution to the kernel done in [11].

The zero binding limit of fig. 6 deserves some comments. It was found in [12] that for massive exchange, the relativistic (BS and LF) ladder results do not coincide with those provided by the Schrödinger equation and the corresponding non relativistic kernel (Yukawa potential) even at very small binding energies. Their differences increase with the exchanged mass μ and do not vanish in the limit $B \to 0$. We have displayed in fig. 7 a zoom of fig. 6 for small values of B. We see from these results that the cross ladder and stretched box diagrams reduce the differences but are not enough to cancel it.

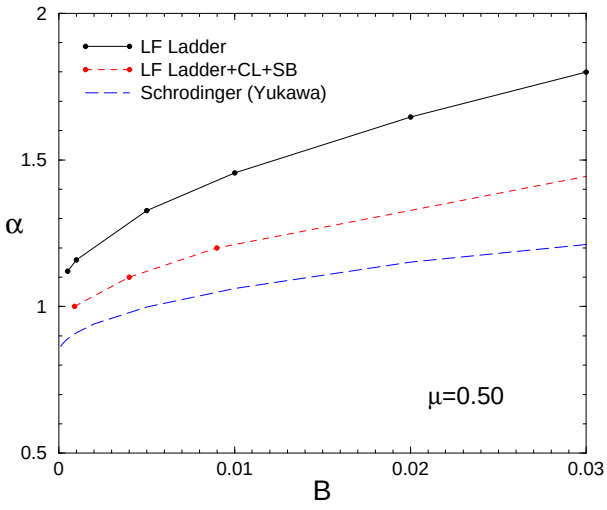

Fig. 7. Zoom of figure 6 in the zero binding energy region. The ladder and (ladder +cross ladder +stretched box) results obtained with the LF equation are compared to the non relativistic ones (Schrodinger equation with Yukawa potential).

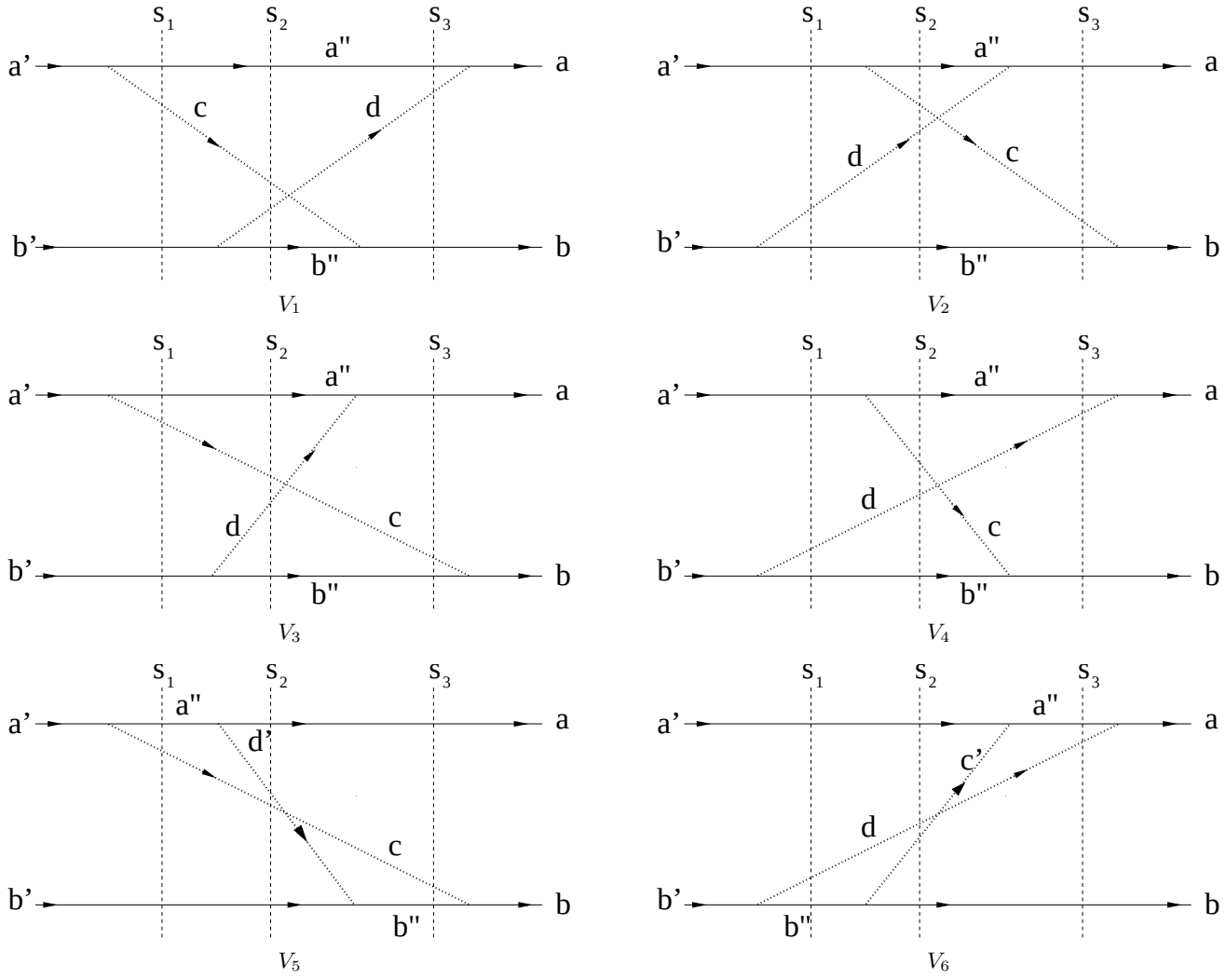

Fig. 3. Cross LFD graphs.

Fig. 4. Stretched boxes.

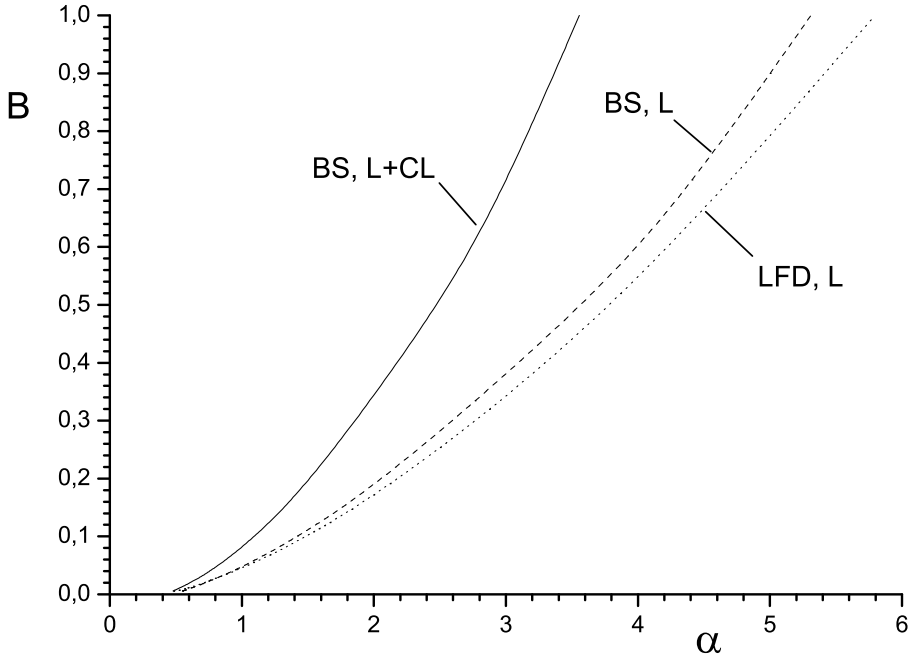

Fig. 5. Binding energy B vs. coupling constant α for BS and LF equations with the ladder (L) kernels only and with the ladder +cross-ladder (L+CL) one for exchange mass $\mu = 0.15$.

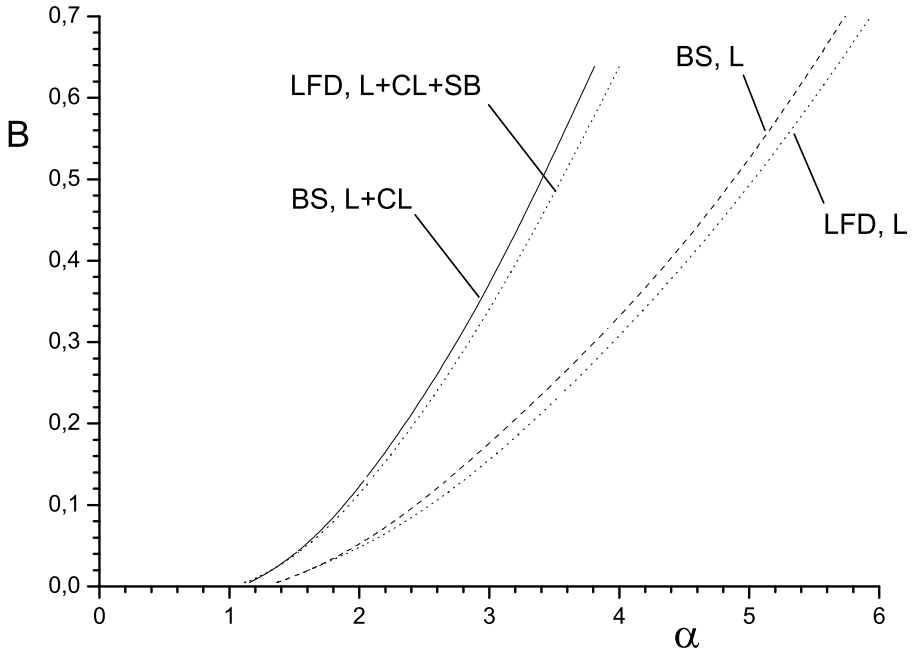

Fig. 6. The same as in fig. 5 for exchange mass $\mu = 0.5$ and, in addition, binding energy B for LF equation with the ladder +cross-ladder +stretched box (L+CL+SB) kernel.

Table 1. Coupling constant α for given values of the binding energy B and exchanged mass $\mu = 0.5$ calculated with BS and LF equations for the ladder (L), ladder +cross-ladder (L+CL) and (in LFD) for the ladder +cross-ladder +stretched-box (L+CL+SB) kernels.

B	BS(L)	BS (L+CL)	LF (L)	LFD (L+CL)	LFD (L+CL+SB)
0.01	1.44	1.21	1.46	1.23	1.21
0.05	2.01	1.62	2.06	1.65	1.62
0.10	2.50	1.93	2.57	2.01	1.97
0.20	3.25	2.42	3.37	2.53	2.47
0.50	4.90	3.47	5.16	3.67	3.61
1.00	6.71	4.56	7.17	4.97	4.91

5 Conclusion

We have solved, for the first time, the BS equation for the kernel given by sum of ladder and cross-ladder exchanges. The solution was found in Minkowski space, i.e. without making use of the Wick rotation, by a new method developed in [1].

In order to compare two different relativistic approaches, we have also solved the corresponding LF equation.

We have found that the cross-ladder contribution, relative to the ladder one, results in a strong attractive effect. The BS and LFD approaches give very close results for any kernel, with BS equation being always more attractive. These approaches differ from each other by the stretched-box diagrams with higher numbers of intermediate mesons. Our results indicate that the higher order stretched box contributions are small. This agrees with direct calculations in LFD of stretched box kernel (fig. 4) with two-meson states [11] and with calculations of the higher Fock sector contributions [13] in the Wick-Cutkosky model. Calculation in LFD of binding energy with the stretched box contribution (L+CL+SB) and its comparison with (L+CL) also shows that the stretched box contribution is attractive but small.

The comparison of our results with those obtained in [5], evaluating the binding energy B_{all} for the complete set of all irreducible diagrams, shows that the effect of the considered cross ladder graphs, though being very important, represent only a small part of the total correction. Thus for $\mu = 0.15$ and $\alpha = 0.9$ the corresponding binding energies obtained with BS equation are $B_L \approx 0.035$, $B_{L+CL} \approx 0.06$ and $B_{all} \approx 0.225$.

We are aware about the only paper [6] where the separated effect of the cross-ladder in the BS framework has been estimated. The method is based on writing an approximate dispersion relation for the kernel. Our results are smaller than the ones found in this reference by a factor 3.

Acknowledgements

Numerical calculations were performed at Institut du Développement et des Ressources en Informatique Scientifique (IDRIS) from CNRS. One of the authors (V.A.K.) is sincerely grateful for the warm hospitality of the theory group at the Laboratoire de Physique Subatomique et Cosmologie, Université Joseph Fourier, in Grenoble, where this work was performed. This work is supported in part by the RFBR grant 05-02-17482-a (V.A.K.).

A Calculating BS cross-ladder

We calculate here the cross-ladder contribution $V^{(CL)}$ to the kernel in eq. (3). We start with the cross-ladder amplitude, eq. (7). Using the Feynman parametrization:

$$\frac{1}{abcd} = 6\int_0^1 dy_3 \int_0^{1-y_3} dy_2 \int_0^{1-y_2-y_3} dy_1 \times \frac{1}{[ay_1 + by_2 + cy_3 + d(1-y_1-y_2-y_3)]^4}$$

and calculating then the integral (7) over p'' in a standard way by means of the formula

$$\int \frac{d^4p''}{(p''^2 + A + i\epsilon)^n} = \frac{i\pi^2}{(n-1)(n-2)(A+i\epsilon)^{n-2}}, \quad (12)$$

we find:

$$K^{(CL)}(k,k',p) = \quad (13)$$
$$16\alpha^2 m^4 \int_0^1 dy_3 \int_0^{1-y_3} dy_2 \int_0^{1-y_2-y_3} dy_1 \; \frac{1}{A'^2},$$

where $\alpha = g^2/(16\pi m^2)$ and

$$\begin{aligned} A' = {} & k'^2\,(y_1+y_3)(1-y_1-y_3) \quad (14)\\ & + k^2\,(y_2+y_3)(1-y_2-y_3)\\ & + k'\cdot p\,\Big(y_1(1-y_1-y_2) - y_3(y_1+y_2)\Big)\\ & - k\cdot p\,\Big(y_2(1-y_1-y_2) - y_3(y_1+y_2)\Big)\\ & + 2k\cdot k'\,\Big((y_1+y_3)(y_2+y_3) - y_3\Big)\\ & + \frac{1}{4}M^2\,(y_1+y_2)(1-y_1-y_2)\\ & - \mu^2\,(1-y_1-y_2) - m^2\,(y_1+y_2) + i\epsilon. \end{aligned}$$

Substituting the kernel (13) in eq. (5), we obtain:

$$I(k,p) = \int \frac{d^4k'}{(2\pi)^4} \frac{iK^{(CL)}(k,k',p)}{H^3} = \int_0^1 dy_3 \int_0^{1-y_3} dy_2 \int_0^{1-y_2-y_3} dy_1 \int \frac{d^4k'}{(2\pi)^4} \frac{16i\alpha^2 m^4}{A'^2\, H^3}, \tag{15}$$

where A' is given by (14) and H is denominator in (5):

$$H = k'^2 + p\cdot k'\; z' - m^2 + \frac{1}{4}M^2 - \gamma' + i\epsilon.$$

Using the formula

$$\frac{1}{A'^2\, H^3} = \int_0^1 \frac{12 y_4(1-y_4)^2 dy_4}{\Big[y_4 A' + (1-y_4)H\Big]^5}$$

and shifting the integration variable k' to eliminate the terms linear in k', we calculate, again by means of eq. (12), the integral (15) over k'. The result is represented in the form:

$$I(k,p) = -\frac{\alpha^2 m^4}{\pi^2} \int \frac{\eta\, y_4(1-y_4)^2 dy_1 dy_2 dy_3 dy_4}{\Big[A(k,p) + i\epsilon\Big]^3} \tag{16}$$

where

$$\eta = 1 - y_4[1 - (1-y_1-y_3)(y_1+y_3)] \tag{17}$$

and $A(k,p)$ depends on $k, p, \gamma', z', y_{1-4}$. We separated the factor η in numerator of (16) so that $A(k,p)$ be a polynomial in all the variables. We do not precise it.

Now we shift the argument k of $I(k,p)$: $k \to k + \beta\omega$, substitute $I(k+\beta\omega, p)$ in eq. (4) for V and replace $\beta' = (\omega\cdot p)\beta$. In addition to the variables γ', z', which enter through eq. (5), the kernel V depends on three scalars k^2, $p\cdot k$ and $\frac{\omega\cdot k}{\omega\cdot p}$: $V = V(k^2, p\cdot k, \frac{\omega\cdot k}{\omega\cdot p}; \gamma', z')$. They vary in the intervals

$$-\infty < k^2 \le 0, \quad -\infty < p\cdot k < \infty, \quad -\frac{1}{2} \le \frac{\omega\cdot k}{\omega\cdot p} \le \frac{1}{2} \tag{18}$$

and satisfy the relation

$$p\cdot k = 2\frac{\omega\cdot k}{\omega\cdot p}\left(k^2 - \kappa^2\right). \tag{19}$$

Therefore, only two of them are independent. We introduce two new variables γ, z related to the three old ones as:

$$k^2 = -\frac{(\gamma + z^2 m^2)}{1-z^2},$$
$$p\cdot k = \frac{z[\gamma + z^2 m^2 + (1-z^2)\kappa^2]}{1-z^2},$$
$$\frac{\omega\cdot k}{\omega\cdot p} = -\frac{1}{2}z.$$

With these definitions, the relation (19) turns into identity and the inequalities (18) are satisfied if γ, z vary in the intervals $0 \le \gamma < \infty$, $-1 \le z \le 1$. So, the kernel V is now parametrized as $V = V(\gamma, z; \gamma', z')$, where γ is in the same interval as γ' and similarly for z, z'. Note that γ, z are related to the standard LF variables $k_\perp, x$ used in sect. 3 as $\gamma = k_\perp^2$, $z = 1 - 2x$.

In this way we get:

$$V^{(CL)}(\gamma, z; \gamma', z') = \frac{-i}{\pi(1-z^2)} \int_{-\infty}^{\infty} I\left(k + \frac{\beta'\omega}{\omega\cdot p}, p\right) \times \frac{d\beta'}{\left(\frac{\gamma + z^2 m^2}{1-z^2} + \kappa^2 - \beta' - i\epsilon\right)\left(\frac{\gamma + z^2 m^2}{1-z^2} + \kappa^2 + \beta' - i\epsilon\right)}. \tag{20}$$

The polynomial $A(k,p)$ determining $I(k,p)$ has the property:

$$A\left(k + \frac{\beta'\omega}{\omega\cdot p}, p\right) = A(k,p) + c_{\beta'}\beta',$$

where $c_{\beta'} = c' y_4(1-z^2)$ and c' is given in appendix A. Therefore the integrand in (20) has two poles of the first order at $\beta' = \beta_\pm$ with

$$\beta_+ = +i\epsilon - \frac{\gamma + z^2 m^2}{1-z^2} - \kappa^2, \quad \beta_- = -i\epsilon + \frac{\gamma + z^2 m^2}{1-z^2} + \kappa^2$$

and one pole of the third order due to the factor

$$\frac{1}{\left[A(k,p) + c_{\beta'}\beta' + i\epsilon\right]^3}.$$

If $c_{\beta'} > 0$ (*i.e.*, $c' > 0$), the third order pole is at $\beta' \sim -i\epsilon$. We close the contour in the upper half-plane and take the residue at $\beta' = \beta_+ \sim +i\epsilon$. If $c' < 0$, this pole is at $\beta' = +i\epsilon$. Then we close the contour in the lower half-plane and take the residue at $\beta' = \beta_- \sim -i\epsilon$. The result reads:

$$V^{(CL)}(\gamma, z; \gamma', z') = \frac{1}{\gamma + m^2 z^2 + \kappa^2(1-z^2)} \times \begin{cases} I(k + \frac{\omega\beta_+}{\omega\cdot p}, p), \text{ if } c' > 0 \\ I(k + \frac{\omega\beta_-}{\omega\cdot p}, p), \text{ if } c' < 0 \end{cases}$$

Substituting here expression (16) for I, we finally find:

$$V^{(CL)}(\gamma, z; \gamma', z') = -\frac{\alpha^2 m^4}{\pi^2} \frac{(1-z^2)^3}{\gamma + m^2 z^2 + \kappa^2(1-z^2)} \times \int_0^1 y_4(1-y_4)^2 dy_4 \int_0^1 dy_3 \int_0^{1-y_3} dy_2 \int_0^{1-y_2-y_3} dy_1 \frac{\eta}{D^3}, \tag{21}$$

η is defined by (17) and D reads:

$$D = c_\gamma \gamma + c_{\gamma'}\gamma' + c_\kappa \kappa^2 + c_m m^2 + c_\mu \mu^2 - y_4 |c'| \Big[\gamma + m^2 z^2 + \kappa^2(1-z^2)\Big]. \tag{22}$$

The coefficients determining D are given below in appendix A.1.

A.1 The coefficients determining D, eq. (22)

$$
\begin{aligned}
c' &= {y_2}^2\ (1+(-1+y_1+y_3)\ y_4)\ (1+z)\\
&+ y_3\ \big({y_1}^2\, y_4\ (-1+z) - (-1+y_3)\ (-1+y_4)\ (z-z')\\
&+ y_1\ (1+y_3\, y_4\ (-1+z) - y_4\, z + (-1+y_4)\ z'))\\
&+ y_2\ ((-1+y_4)\ (1+z)\\
&+ {y_1}^2\, y_4\ (1+z) + {y_3}^2\, y_4\ (1+z)\\
&+ y_3\ (1+2\,z - z' + y_4\ (-2-3\,z+z'))\\
&+ y_1\ (1-z'+y_4\ (-2-z+2\,y_3\ (1+z)+z')))
\end{aligned}
$$

$$
\begin{aligned}
c_\gamma &= y_4\ \big({y_2}^2\ (1+(-1+y_1+y_3)\ y_4)\ (1+z)\\
&+ y_3\ (-1+y_3+(1+(-1+y_1)\ y_1)\ y_4\\
&- y_3\, y_4 + y_1\, y_3\, y_4 + y_1\, z - {y_1}^2\, y_4\, z - y_1\, y_3\, y_4\, z\\
&+ (-1+y_1+y_3)\ (-1+y_4)\ z\, z')\\
&+ y_2\ (-1+(1+(-1+y_1)\ y_1)\ y_4\ - z\\
&+ {y_3}^2\, y_4\ (1+z)\\
&+ y_3\ (2+z+y_4\ (-3-2\,z+2\,y_1\ (1+z))\\
&+ (-1+y_4)\ z\, z')\\
&+ z\ (y_4+y_1\ (1-z'+y_4\ (-2+y_1+z')))))
\end{aligned}
$$

$$
\begin{aligned}
c_{\gamma'} &= (-1+y_4)\ \big(-1+\big(1+{y_1}^2+(-1+y_3)\ \ y_3\\
&+\ y_1\ (-1+2\,y_3))\ y_4)\ \big(-1+z^2\big)
\end{aligned}
$$

$$
\begin{aligned}
c_\kappa &= -\Big(\big(-1+z^2\big)\ \Big(-1+{z'}^2+y_4\ (2+(-1+y_3)\ y_3\\
&+\ \ y_2\ (-1+y_2+(-1+y_2+y_3)\ z)\\
&- 2\,{y_1}^2\ (-1+z') - y_1\ (-2+y_2\ (2+z)\\
&+\ y_3\ (2+z))\ (-1+z')\\
&-\ \ y_3\ (2\,y_2+(-1+y_2+y_3)\ z)\ z' - 2\,{z'}^2\Big)\\
&+ {y_4}^2\ \big(-1+y_2+y_3-{y_3}^2+{y_2}^2\ (-1+y_3)\ (1+z)\\
&+ y_2\ (-1+y_3)\ (y_3+(-1+y_3)\ z)\\
&+ (-1+y_3)\ y_3\, z\, z' + y_2\, y_3\ (2+z)\ z' + {z'}^2\\
&+\ \ {y_1}^2\ (-2+y_2+y_3+y_2\, z - y_3\, z + 2\,z')\\
&+ y_1\ \big(2+{y_2}^2\ (1+z) - 2\,z'\\
&+ y_3\ (-3+y_3-y_3\, z+(2+z)\ z')\\
&+\ \ y_2\ (-3-2\,z+2\,y_3\ (1+z)+(2+z)\ z')))))
\end{aligned}
$$

$$
\begin{aligned}
c_m &= -\big({y_1}^3\, {y_4}^2\ \big(-1+z^2\big)\big)\\
&+ {y_2}^2\, y_4\ (1+(-1+y_3)\ y_4)\ (1+z)\ \big(-1+z+z^2\big)\\
&+ {y_1}^2\, y_4\ \big((1+z)\ \big(-1+z+y_2\, y_4\, z^2\big)\\
&+ y_3\ \big(y_4 - y_4\, z^3\big) + 2\ (-1+y_4)\ \big(-1+z^2\big)\ z'\big)\\
&+ y_2\, y_4\ \big(z^2\ (-1+y_4+y_3\ (2+(-3+y_3)\ y_4)\\
&-\ \ z + \Big(y_3+(-1+y_3)^2\, y_4\Big)\ z\Big)\\
&+ y_3\ (-1+y_4)\ \big(-2+z^2\ (2+z)\big)\ z'\big)\\
&+ (-1+y_4)\ \big(-\big((-1+y_3)\ y_3\, y_4\, z^2\big)\\
&+\ (-1+y_3)\ y_3\, y_4\, z^3\, z' + (-1+y_4)\ \big(-1+z^2\big)\ {z'}^2\big)\\
&+ y_1\, y_4\ \big(-\big(y_3\ (y_4\ (1+y_3\ (-1+z))-z)\ z^2\big)\\
&+ {y_2}^2\, y_4\ (1+z)\ \big(-1+z+z^2\big)\\
&+ (-1+y_4)\ \big(2-2\,z^2+y_3\ \big(-2+z^2\ (2+z)\big)\big)\ z'\\
&+ y_2\ \big(-\big(\big(-2+z^2\ (2+z)\big)\ (-1+z')\big)\\
&+ y_4\ \big(2-2\,z'+z^2\ (-3-2\,z+2\,y_3\ (1+z)\\
&+\ \ (2+z)\ z'))))
\end{aligned}
$$

$$
\begin{aligned}
c_\mu &= (-1+y_1+y_2)\ y_4\ \big(-1+\big(1+{y_1}^2+(-1+y_3)\ y_3\\
&+\ \ y_1\ (-1+2\,y_3))\ y_4)\ \big(-1+z^2\big)
\end{aligned}
$$

B Calculating LFD cross-ladders

At first we will transform the 3-dim. LF equation (8) in a 2-dim. form. The kernel $V_{LF}(\boldsymbol{k'}_\perp, x'; \boldsymbol{k}_\perp, x, M^2)$ depends on the scalar product

$$\boldsymbol{k}_\perp \cdot \boldsymbol{k'}_\perp = k_\perp k'_\perp \cos\phi'.$$

Since $\psi(\boldsymbol{k'}_\perp, x)$ depends on $|\boldsymbol{k'}_\perp| \equiv k'_\perp$ and does not depend on the angle ϕ', one can integrate the kernel over ϕ' and the equation (8) turns into:

$$
\begin{aligned}
&\left(\frac{k_\perp^2+m^2}{x(1-x)} - M^2\right)\psi(k_\perp, x) = \qquad (23)\\
&-\frac{m^2}{2\pi^3}\int \psi(k'_\perp, x')\tilde{V}_{LF}(k'_\perp, x', k_\perp, x, M^2)\frac{k'_\perp\, dk'_\perp\, dx'}{2x'(1-x')},
\end{aligned}
$$

where

$$\tilde{V}_{LF}(k'_\perp, x', k_\perp, x, M^2) = \int_0^{2\pi} V_{LF}(\boldsymbol{k'}_\perp, x', \boldsymbol{k}_\perp, x, M^2)d\phi'. \qquad (24)$$

To calculate the kernel in the LF equation (8), one can use the Weinberg rules [14], which are equivalent to the graph techniques in LFD [10]. To calculate the amplitude $-\mathcal{M}$, one should put in correspondence: to every vertex – the factor g, to every intermediate state – the factor,

$$\frac{2}{s_0 - s_{int} + i0}, \quad \text{where} \quad s_{int} = \sum_i \frac{\boldsymbol{k}_{i\perp}^2 + m_i^2}{x_i}$$

and s_0 is the initial (=final) state energy. In our case (bound state): $s_0^2 = M^2$. To every internal line one should put in correspondence the factor $\frac{\theta(x_i)}{2x_i}$. One should take into account the conservation laws for $\boldsymbol{k}_{i\perp}$ and x_i in any vertex and integrate over all independent variables with the measure $\frac{d^2k_{i\perp}\,dx_i}{(2\pi)^3}$.

Applied to the ladder graphs fig. 2, these rules result in eq. (9) for the ladder contribution. The integral (24) is calculated analytically.

There are six cross-ladder time-ordered diagrams shown in fig. 3. Sum of them determines, by eq. (10), the kernel $V_{LF}^{(CL)}$. Consider four diagrams for V_{1-4} in fig. 3. They

contain eight lines $(a', a'', a, b', b'', b, c, d)$ and three intermediate states. The momenta corresponding to these lines are the following:

$$\begin{array}{ll}
(a') & \boldsymbol{k'}_\perp,\ x' \\
(a'') & \boldsymbol{k''}_\perp,\ x'' \\
(a) & \boldsymbol{k}_\perp,\ x \\
(b') & -\boldsymbol{k'}_\perp,\ 1-x' \\
(b'') & \boldsymbol{k''}_\perp - \boldsymbol{k'}_\perp - \boldsymbol{k}_\perp,\ 1+x''-x'-x \\
(b) & -\boldsymbol{k}_\perp,\ 1-x \\
(c) & \boldsymbol{k'}_\perp - \boldsymbol{k''}_\perp,\ x'-x'' \\
(d) & \boldsymbol{k}_\perp - \boldsymbol{k''}_\perp,\ x-x''
\end{array}$$

Introduce for every line the energy:

$$\begin{aligned}
E_{a'} &= \frac{\boldsymbol{k'}_\perp^2 + m^2}{x'} \\
E_{a''} &= \frac{\boldsymbol{k''}_\perp^2 + m^2}{x''} \\
E_a &= \frac{\boldsymbol{k}_\perp^2 + m^2}{x} \\
E_{b'} &= \frac{\boldsymbol{k'}_\perp^2 + m^2}{1-x'} \\
E_{b''} &= \frac{(\boldsymbol{k''}_\perp - \boldsymbol{k'}_\perp - \boldsymbol{k}_\perp)^2 + m^2}{1+x''-x'-x} \\
E_b &= \frac{\boldsymbol{k}_\perp^2 + m^2}{1-x} \\
E_c &= \frac{(\boldsymbol{k'}_\perp - \boldsymbol{k''}_\perp)^2 + \mu^2}{x'-x''}; \\
E_d &= \frac{(\boldsymbol{k}_\perp - \boldsymbol{k''}_\perp)^2 + \mu^2}{x-x''}.
\end{aligned}$$

Energies in three intermediate states for V_1 are written as:

$$\begin{aligned}
s_1 &= E_{a''} + E_c + E_{b'}, \\
s_2 &= E_{a''} + E_c + E_d + E_{b''}, \\
s_3 &= E_{a''} + E_d + E_b.
\end{aligned}$$

The kernel V_{LF} is related to the amplitude $\mathcal{M}$ as: $V_{LF} = -\mathcal{M}/(4m^2)$. For the diagram fig. 3,V_1 it has the form:

$$V_1 = -\int \frac{g^4\theta(x'')\theta(x-x'')\theta(x'-x'')\theta(1+x''-x-x')}{4m^2(s_1-M^2)(s_2-M^2)(s_3-M^2)} \times \frac{1}{x''(x-x'')(x'-x'')(1+x''-x-x')} \frac{d^2k''_\perp dx''}{2(2\pi)^3}. \tag{25}$$

Since:

$$\begin{aligned}
\boldsymbol{k}_\perp \cdot \boldsymbol{k'}_\perp &= k_\perp k'_\perp \cos\phi', \\
\boldsymbol{k}_\perp \cdot \boldsymbol{k''}_\perp &= k_\perp k''_\perp \cos\phi'', \\
\boldsymbol{k'}_\perp \cdot \boldsymbol{k''}_\perp &= k'_\perp k''_\perp \cos(\phi'-\phi''),
\end{aligned}$$

the integrand depends on two azimuthal angles ϕ', ϕ''. The kernel (25) is determined by the 3-dim. integral over $d^2k''_\perp dx'' = k''_\perp dk''_\perp d\phi'' dx''$. Therefore the contribution of fig. 3,V_1 to the kernel $\tilde{V}_{LF}$, eq. (24), is determined by a 4-dim. integral:

$$\tilde{V}_1(k'_\perp, x', k_\perp, x, M^2) = \int_0^{2\pi} V_1(\boldsymbol{k'}_\perp, x', \boldsymbol{k}_\perp, x, M^2) d\phi'$$
$$= \int_{max(0,x+x'-1)}^{min(x,x')} dx'' \int \frac{-4m^2\alpha^2 k''_\perp dk''_\perp d\phi'' d\phi'}{\pi(s_1-M^2)(s_2-M^2)(s_3-M^2)} \times \frac{1}{x''(x-x'')(x'-x'')(1+x''-x-x')} \tag{26}$$

with $\alpha = g^2/(16\pi m^2)$. We have removed the theta-functions and incorporated the integration limits in the variable x'' explicitly. One can calculate the 4-dim. integral (26) for the kernel numerically.

Consider now another three kernels V_2, V_3, V_4 shown in figs. 3. They still have the form (26), but the corresponding energies s_1, s_2, s_3 are different.

We denote the kernel corresponding to fig. 3, V_2, after integration over ϕ', as $\tilde{V}_2(k'_\perp, x', k_\perp, x, M^2)$. It has exactly the same form as eq. (26), but with energies given by:

$$\begin{aligned}
s_1 &= E_{a'} + E_d + E_{b''}, \\
s_2 &= E_{a''} + E_c + E_d + E_{b''}, \\
s_3 &= E_a + E_c + E_{b''}.
\end{aligned}$$

The kernel $\tilde{V}_3(k'_\perp, x', k_\perp, x, M^2)$ corresponding to the graph fig. 3, V_3 has exactly the same form as eq. (26), but with energies given by:

$$\begin{aligned}
s_1 &= E_{a''} + E_c + E_{b'}, \\
s_2 &= E_{a''} + E_c + E_d + E_{b''}, \\
s_3 &= E_a + E_c + E_{b''}.
\end{aligned}$$

The kernel $\tilde{V}_4(k'_\perp, x', k_\perp, x, M^2)$ corresponding to the graph fig. 3, V_4 also has exactly the same form as eq. (26), but with energies given by:

$$\begin{aligned}
s_1 &= E_{a'} + E_d + E_{b''}, \\
s_2 &= E_{a''} + E_c + E_d + E_{b''}, \\
s_3 &= E_{a''} + E_d + E_b.
\end{aligned}$$

Another two cross-ladder graphs are shown in figs. 3, V_5 and V_6. Here we have new lines d', c'. Corresponding momenta and energies are the following:

$$\begin{array}{ll}
(d') & \boldsymbol{k''}_\perp - \boldsymbol{k}_\perp,\ x''-x \\
(c') & \boldsymbol{k''}_\perp - \boldsymbol{k'}_\perp,\ x''-x'
\end{array}$$

$$\begin{aligned}
E_{d'} &= \frac{(\boldsymbol{k''}_\perp - \boldsymbol{k}_\perp)^2 + \mu^2}{x''-x} = -E_d\ , \\
E_{c'} &= \frac{(\boldsymbol{k''}_\perp - \boldsymbol{k'}_\perp)^2 + \mu^2}{x''-x'} = -E_c\ .
\end{aligned}$$

If $x' > x$, only V_5 contributes. It has the form:

$$\tilde{V}_5 = \int_x^{x'} dx'' \int \frac{-4m^2\alpha^2\ d^2k''_\perp d\phi'}{\pi(s_1-M^2)(s_2-M^2)(s_3-M^2)} \times \frac{\theta(x'-x)}{x''(x''-x)(x'-x'')(1+x''-x-x')} \tag{27}$$

with s_1, s_2, s_3 given by:

$$s_1 = E_{a''} + E_c + E_{b'},$$
$$s_2 = E_a + E_c + E_{d'} + E_{b'},$$
$$s_3 = E_a + E_c + E_{b''}.$$

If $x > x'$, only V_6 contributes. It has the form:

$$\tilde{V}_6 = \int_{x'}^{x} dx'' \int \frac{-4m^2\alpha^2 d^2k''_\perp d\phi'}{\pi(s_1 - M^2)(s_2 - M^2)(s_3 - M^2)} \times \frac{\theta(x - x')}{x''(x - x'')(x'' - x')(1 + x'' - x - x')} \qquad (28)$$

with s_1, s_2, s_3 given by:

$$s_1 = E_{a'} + E_d + E_{b''},$$
$$s_2 = E_{a'} + E_{c'} + E_d + E_b,$$
$$s_3 = E_{a''} + E_d + E_b.$$

B.1 Test by the Feynman cross graph

On the energy shell the sum of six contributions $V^{(CL)} = \sum_{i=1}^{6} V_i$, fig. 3, must coincide with the value of the Feynman cross graph, fig. 1, taken on the mass shell, namely, with

$$V^{(CL)}_{Feyn} = -\frac{1}{4m^2} K^{(CL)}(k, k', p).$$

$K^{(CL)}(k, k', p)$ is given by (13) where in the denominator A', eq. (14), one should put

$$M^2 = s, \quad k^2 = k'^2 = m^2 - \frac{1}{4}s,$$
$$k \cdot p = k' \cdot p = 0, \quad k \cdot k' = m^2 - \frac{1}{4}s - \frac{1}{2}t$$

and s, t are in the physical domain. Expression (14) is considerably simplified and we find:

$$V^{(CL)}_{Feyn} = -4\alpha^2 m^2 \int_0^1 dy_3 \int_0^{1-y_3} dy_2 \int_0^{1-y_2-y_3} dy_1 \times \Big[(1 - y_1 - y_2)(\mu^2 - y_3 t) + (y_1 - y_2)^2 m^2 + y_3^2 t + y_1 y_2 (s + t)\Big]^{-2}. \qquad (29)$$

The 3-dim. integral (29) is calculated numerically. One can chose a particular kinematics, for example, in c.m.-frame, where s and t for elastic scattering are determined by incident (=final) momentum and the scattering angle.

On the other hand, we calculate the sum of six LF cross graphs

$$V^{(CL)}_{LF}(\boldsymbol{k'}_\perp, x', \boldsymbol{k}_\perp, x, M^2 = s) = \sum_{i=1}^{6} V_i$$

(not integrated over ϕ'). Here

$$x = \frac{\omega \cdot p_1}{\omega \cdot (p_1 + p_2)}, \quad x' = \frac{\omega \cdot p'_1}{\omega \cdot (p_1 + p_2)}$$

and $\boldsymbol{k}_\perp, \boldsymbol{k'}_\perp$ are projections of $\boldsymbol{p}_1$, $\boldsymbol{p'}_1$ on the plane orthogonal to $\boldsymbol{\omega}$. We remind that $\omega = (\omega_0, \boldsymbol{\omega})$ is an arbitrary four-vector with $\omega^2 = 0$. Though, for a given kinematics, the values of $\boldsymbol{k}_\perp, x, \boldsymbol{k'}_\perp, x'$ depend on orientation of $\boldsymbol{\omega}$, the on-shell amplitude $V^{(CL)}_{LF}(\boldsymbol{k'}_\perp, x', \boldsymbol{k}_\perp, x, M^2 = s)$ does not depend on it. We can chose $\omega = (1, 0, 0, -1)$, find the arguments of $V^{(CL)}_{LF}(\boldsymbol{k'}_\perp, x', \boldsymbol{k}_\perp, x, M^2 = s)$ in kinematics for the c.m. elastic scattering and calculate $V^{(CL)}_{LF}$.

For different incident momenta and scattering angles we have checked numerically that $V^{(CL)}_{Feyn}$, eq. (29), coincides with the sum of six cross graphs $V^{(CL)}_{LF} = \sum_{i=1}^{6} V_i$. This confirms validity of both calculations.

C Calculating LFD stretched boxes

The stretched-box graphs determine the kernel $V^{(SB)}_{LF}$, eq. (10). They are shown in fig. 4 and their contributions are denoted as V_7 and V_8. We introduce the line b'''. All the momenta except for the line b''' are the same as for the cross graphs. The momentum and energy carried by the lines b''' are the following:

$$(b''') \quad -\boldsymbol{k''}_\perp, \ 1 - x''$$
$$E_{b'''} = \frac{\boldsymbol{k''}^2_\perp + m^2}{1 - x''}$$

The following product of the theta-functions enters the kernel V_7

$$\theta(x'')\theta(x'' - x)\theta(x' - x'')\theta(1 - x'').$$

It restricts the integration domain as:

$$0 \le x \le x'' \le x' \le 1.$$

Therefore the kernel $\tilde{V}_7$ is nonzero at $x' > x$ only. It has the form:

$$\tilde{V}_7 = \int_{x}^{x'} dx'' \int \frac{-4m^2\alpha^2 \ d^2k''_\perp d\phi'}{\pi(s_1 - M^2)(s_2 - M^2)(s_3 - M^2)} \times \frac{\theta(x' - x)}{x''(x'' - x)(x' - x'')(1 - x'')} \qquad (30)$$

The corresponding energies s read:

$$s_1 = E_{a''} + E_c + E_{b'},$$
$$s_2 = E_a + E_{d'} + E_c + E_{b'},$$
$$s_3 = E_a + E_{d'} + E_{b'''}$$

and the energies E are given above in appendix B and in this appendix.

The kernel $\tilde{V}_8$ is non-zero at $x' < x$ only. It has the form:

$$\tilde{V}_8 = \int_{x'}^{x} dx'' \int \frac{-4m^2\alpha^2 \ d^2k''_\perp d\phi'}{\pi(s_1 - M^2)(s_2 - M^2)(s_3 - M^2)} \times \frac{\theta(x - x')}{x''(x - x'')(x'' - x')(1 - x'')} \qquad (31)$$

with s_1, s_2, s_3 given by:

$$s_1 = E_{a'} + E_{c'} + E_{b'''},$$
$$s_2 = E_{a'} + E_{c'} + E_d + E_b,$$
$$s_3 = E_{a''} + E_d + E_b.$$

References

1. V.A. Karmanov and J. Carbonell, Eur. Phys. J. **A 27** (1), 1 (2006); hep-th/0505261.
2. E.E. Salpeter and H.A. Bethe, Phys. Rev. **84**, 1232 (1951).
3. G.C. Wick, Phys. Rev. **96**, 1124 (1954); R.E. Cutkosky, Phys. Rev. **96**, 1135 (1954).
4. K. Kusaka, A.G. Williams, Phys. Rev. **D 51**, 7026 (1995); K. Kusaka, K. Simpson, A.G. Williams, Phys. Rev. **D 56**, 5071 (1997).
5. T. Nieuwenhuis and J.A. Tjon, Phys. Rev. Lett. 77, 814 (1996).
6. A. Amghar, B. Desplanques and L. Theusl, Nucl. Phys. **A 694**, 439 (2001).
7. C.R. Ji, Phys. Lett. **B 322**, 389 (1994); C.R. Ji, G.H. Kim, D.P. Min, Phys. Rev. **D 51**, 879 (1995).
8. V. Sauli, J. Adam, Phys. Rev. **D 67**, 085007 (2003).
9. N. Nakanishi, Phys. Rev. **130**, 1230 (1963); Prog. Theor. Phys. Suppl. 43, 1 (1969); *Graph Theory and Feynman Integrals* (Gordon and Breach, New York, 1971).
10. J. Carbonell, B. Desplanques, V.A. Karmanov and J.-F. Mathiot, Phys. Reports, **300**, 215 (1998).
11. N.C.J. Schoonderwoerd, B.L.G. Bakker and V.A. Karmanov, Phys. Rev. **C 58**, 3093 (1998).
12. M. Mangin-Brinet and J. Carbonell, Phys. Lett., **B 474**, 237 (2000).
13. D.S. Hwang and V.A. Karmanov, Nucl. Phys., **B 696**, 413 (2004).
14. S. Weinberg, Phys. Rev. **150**, 1313 (1966).